Article

A monotreme-like auditory apparatus in a Middle Jurassic haramiyidan

Junyou Wang[1,2], John R. Wible[1,3 ✉], Bin Guo[2], Sarah L. Shelley[3,6], Han Hu[4] & Shundong Bi[1,5 ✉]

Among extant vertebrates, mammals are distinguished by having a chain of three auditory ossicles (the malleus, incus and stapes) that transduce sound waves and promote an increased range of audible—especially high—frequencies[1]. By contrast, the homologous bones in early fossil mammals and relatives also functioned in chewing through their bony attachments to the lower jaw[2]. Recent discoveries of well-preserved Mesozoic mammals have provided glimpses into the transition from the dual (masticatory and auditory) to the single auditory function for the ossicles, which is now widely accepted to have occurred at least three times in mammal evolution[3–6]. Here we report a skull and postcranium that we refer to the haramiyidan *Vilevolodon diplomylos* (dating to the Middle Jurassic epoch (160 million years ago)) and that shows excellent preservation of the malleus, incus and ectotympanic (which supports the tympanic membrane). After comparing this fossil with other Mesozoic and extant mammals, we propose that the overlapping incudomallear articulation found in this and other Mesozoic fossils, in extant monotremes and in early ontogeny in extant marsupials and placentals is a morphology that evolved in several groups of mammals in the transition from the dual to the single function for the ossicles.

In the past 25 years, new discoveries of Mesozoic mammals and their near relatives (Mammaliaformes) have substantially increased our understanding of early mammal evolution[7,8]. Among the most note-worthy and well-preserved finds are those of haramiyidans from the Middle Jurassic Tiaojishan Formation of China, which have molars with multiple cusps in rows and include three gliders (as reconstructed from impressions of patagia)[3,4,9–12]. Along with increased knowledge of the Tiaojishan haramiyidans has come controversy regarding interpretations of their morphology (including of the middle ear) and its effect on their phylogenetic relationships.

Three middle-ear morphologies—which are usually termed mandibular, transitional and definitive mammalian[13,14]—have been reported for mammaliaform (Fig. 1). These terms are not descriptive[15]; for example, definitive mammalian is not present in all members of Mammalia. Here we propose terms grounded in morphology. The first type (Fig. 1a) represents the ancestral condition that is present in nonmammaliaform cynodonts. This type reconstructs the postdentary bones (including the homologues of the malleus and ectotympanic of extant mammals) and Meckel's cartilage within a postdentary trough and Meckelian sulcus on the medial surface of the mandible. We therefore refer to it as the postdentary-attached middle ear (corresponding to the mandibular middle ear[2]), in which auditory functions are coupled with mastication. In the second type (Fig. 1b), the postdentary trough is absent in adults and the postdentary bones are attached to the mandible through only Meckel's cartilage in the Meckelian sulcus. We refer to it as the Meckelian-attached middle ear: this type encompasses the transitional middle ear[14], in which the attachment is specifically through an ossified

Meckel's element. In the third type (Fig. 1c), which is present in all extant adult mammals, the postdentary bones lack a bony or cartilaginous attachment to the mandible and have an exclusive auditory function: we refer to this as the detached middle ear[15] (corresponding to the definitive mammalian middle ear[2]).

Of these three types of middle ear, the postdentary-attached and detached have been reconstructed in different Tiaojishan haramiyidans. Phylogenetic analyses that use the postdentary-attached interpretation, which is based on *V. diplomylos*[4], place the Tiaojishan haramiyidans outside of crown Mammalia[4,16] (Extended Data Fig. 1a). By contrast, phylogenetic analyses that use the detached interpretation—based largely on *Arboroharamiya allinhopsoni*[3,17]—place the Tiaojishan haramiyidans within crown Mammalia[3,5,6] (Extended Data Fig. 1b). The position of this grouping and its relationship to the Late Triassic haramiyidans *Haramiyavia*[18] and *Thomasia*[19] affect our views on the timing of the origin of crown Mammalia, which range between the middle Late Triassic and late Early Jurassic epochs—a difference of 30 million years.

Reinterpretation of haramiyidan ear ossicles

Vilevolodon diplomylos is central to this controversy. This gliding mammal was named from a single relatively complete skull and post-cranial skeleton found in the Middle Jurassic Tiaojishan Formation of northeastern China[4]. In this specimen, much of the auditory ossicular chain is preserved bilaterally but both sides are fragmentary and displaced. Here we report a second nearly complete skull and post-cranial skeleton (accessioned as Inner Mongolia Museum of Natural

[1]Centre for Vertebrate Evolutionary Biology, Institute of Palaeontology, Yunnan University, Kunming, China. [2]Inner Mongolia Museum of Natural History, Hohhot, China. [3]Section of Mammals, Carnegie Museum of Natural History, Pittsburgh, PA, USA. [4]Zoology Division, School of Environmental and Rural Sciences, University of New England, Armidale, New South Wales, Australia. [5]Department of Biology, Indiana University of Pennsylvania, Indiana, PA, USA. [6]Present address: School of Geosciences, University of Edinburgh, Edinburgh, UK. ✉e-mail: WibleJ@CarnegieMNH.org; shundong.bi@iup.edu

a Postdentary-attached — *Morganucodon*

b Meckelian-attached — *Liaoconodon*

c Detached — *Vilevolodon*

Meckelian sulcus   Postdentary trough   Meckelian sulcus

■ Incus (quadrate)   ■ Malleus (articular)   ■ Surangular   ■ Meckel's cartilage   ■ Ectotympanic (angular)
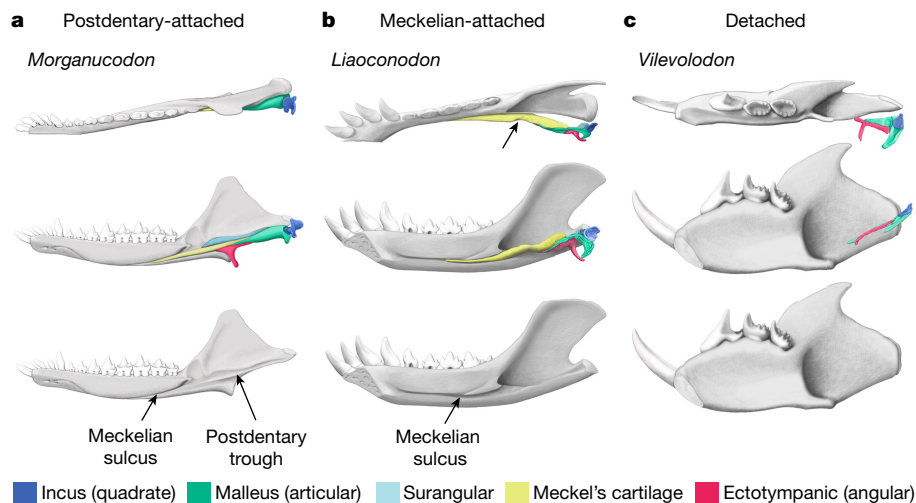
Fig. 1 | Three types of middle ear in mammaliaforms. Mandibles and auditory elements (excluding stapes) in occlusal and medial views. **a**, In the postdentary-attached middle ear, the postdentary bones and Meckel's cartilage are attached to the mandible via the postdentary trough and Meckelian sulcus (Late Triassic–Early Jurassic mammaliaform *Morganucodon*, based on refs. [13,45]). **b**, In the Meckelian-attached middle ear, the postdentary trough is absent and the postdentary bones are attached to the mandible via Meckel's cartilage (ossified in this example) in the Meckelian sulcus; Meckel's element is bent medially (arrow), moving the postdentary bones away from the temporomandibular joint (Early Cretaceous eutriconodontan *Liaoconodon*, based on refs. [6,14,22]). **c**, In the detached middle ear, the postdentary trough and Meckelian sulcus are absent and the auditory elements are detached from the mandible (Middle Jurassic haramiyidan *Vilevolodon*, as reported in this Article).

History (IMMNH)-PV01699) from the same locality and geological formation as the holotype: we refer this material to *V. diplomylos* (Fig. 2, Extended Data Figs. 2, 3, Supplementary Information). In contrast to the holotype, the ossicular chain in IMMNH-PV01699 is well-preserved and in near-life position, which enables us to address issues raised by the more-fragmentary auditory apparatus of the holotype as well as that reconstructed for other Tiaojishan haramiyidans (Extended Data Figs. 4–6, Supplementary Information).

The complete incus, malleus, ectotympanic and the mandible are preserved on the surface of the main slab of IMMNH-PV01699 (Fig. 2a); we used computed tomography scans to supplement the surface view. Both the left and right incus are in articulation with their respective malleus and the left ectotympanic is in near-life position next to the left malleus, all in dorsal view (Fig. 2b, c). The medial surface of the mandible in IMMNH-PV01699 is clearly without a postdentary trough or Meckelian sulcus (Figs. 1c, 2c, Extended Data Fig. 3e), the condition reported for all other Tiaojishan haramiyidans[3,9,10,12,20] except the *Vilevolodon* holotype[4]—which is contradicted by the well-preserved IMMNH-PV01699. As it has no postdentary trough or Meckelian sulcus, the middle ear of IMMNH-PV01699 is of the detached type (Fig. 1c). The left ectotympanic (Fig. 2d, e) has three prongs, a long posterior limb and subequal anterior limb and reflected lamina, and a shallow attachment area for the tympanic membrane (Extended Data Fig. 5f). The malleus has a flattened body and an anterior process (prearticular) but lacks an ossified Meckel's cartilage or surangular (an accessory postdentary bone), both of which were reconstructed on the fragmentary malleus of the holotype[4] (Extended Data Fig. 4). The mallear body is sickle-shaped with the pointed manubrium curving anteriorly and, in life, contacting the tympanic membrane; the dorsal surface of the body includes the gently concave incudal articular facet (Fig. 2d). The mallear anterior process tapers distally parallel to, and with a contact surface for, the posterior limb of the ectotympanic. The incus is flat with a gently convex articular surface and triangular with a process at each angle: a slightly elevated stapedial process (crus longum), a blunt short process (crus breve) that probably contacted the petrosal bone on the skull base and an anterior prominence.

Following our reinterpretation of *Vilevolodon*, all Tiaojishan haramiyidans that preserve the medial surface of the mandible lack a

postdentary trough and Meckelian sulcus[3,9,10,12,20], and can be reconstructed with a detached middle ear. Although isolated auditory elements are known for several Tiaojishan haramiyidans[4,12,20], only *A. allinhopsoni* has been reported to preserve all of the auditory elements (Extended Data Fig. 5a). However, the reconstruction that was previously proposed for them[3,17] is built on a pattern unlike that of *Vilevolodon* or any other mammaliaform (Extended Data Fig. 5b, c). The widespread pattern in mammaliaforms is to have strong support for the tympanic membrane formed by the posterior crus (limb) of the ectotympanic (angular) buttressed by the anterior process of the malleus (prearticular) and to have the opposite side of the tympanic membrane, with the manubrium and the anterior crus (reflected lamina), more open (Fig. 3, Extended Data Fig. 5d). By contrast, in the *A. allinhopsoni* reconstruction[3,17], both the posterior limb and anterior process of the malleus are reduced and do not contact, and the opposite side of the tympanic membrane is well-supported by a neomorphic medial process of the malleus that contacts the ectotympanic (Extended Data Fig. 5b, c). Additionally, the bone reconstructed as the ectotympanic in *A. allinhopsoni* is sickle-shaped[3,17] in contrast to the three-pronged element in *Vilevolodon* and other extinct nontherian mammaliaforms (Fig. 1a, b) or the more ring-shaped element in extant monotremes and many extant therians (marsupials and placentals) (Fig. 3b, h, Extended Data Fig. 5d, g). An isolated bone of *A. allinhopsoni* that has one robust and one needle-like end is purported to be a surangular[3,17] (Extended Data Fig. 5a–c), a postdentary bone that is broadly present in nonmammalian cynodonts[2] but is present in only a few instances in extinct mammaliaforms[5,6,21,22] (Supplementary Information). The bone in question bears little resemblance to any surangular, which is invariably in broad sutural contact with other elements of the auditory apparatus—contact that is lacking in the *A. allinhopsoni* 'surangular'. Informed by the morphology of the specimen we refer to *Vilevolodon*, we reinterpret the auditory apparatus of *A. allinhopsoni* to fit the pattern that is broadly present across Mesozoic mammaliaforms (Extended Data Fig. 5d–i, Supplementary Information).

Phylogenetic analysis using parsimony with the information from IMMNH-PV01699 places *Vilevolodon* in a haramiyidan clade that includes seven other species from the Tiaojishan Formation, along with dental and gnathic taxa from the Late Triassic epoch of Europe[19],
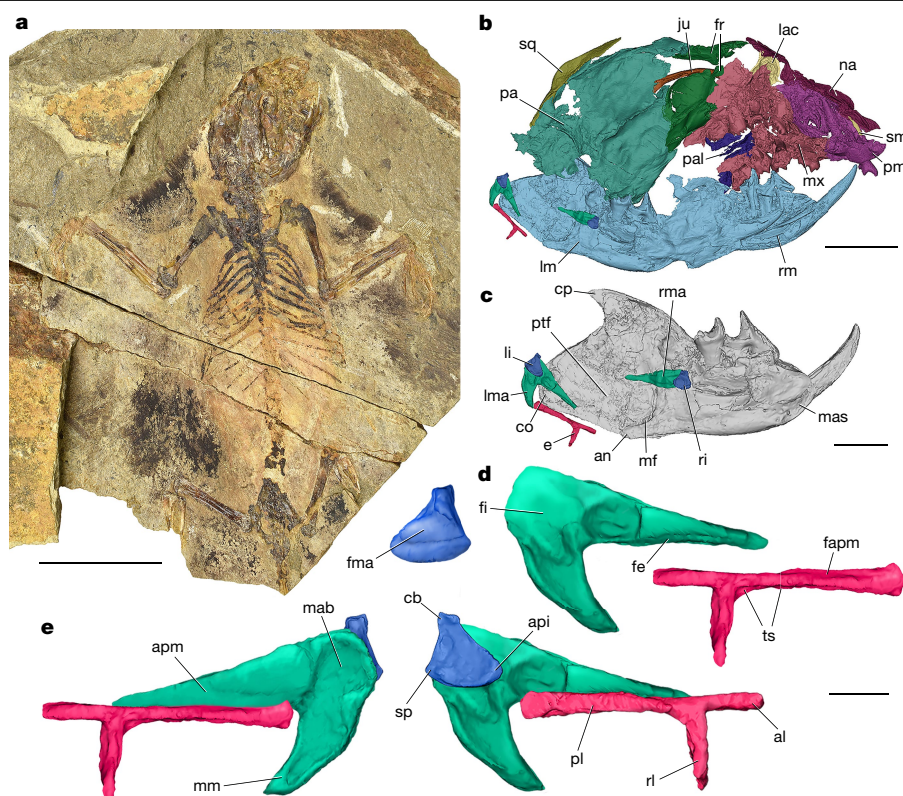
Fig. 2 | *Vilevolodon diplomylos* (IMMNH-PV01699A). a, Main slab; dark patches outside the skeleton between the skull, forelimbs and hind limbs indicate the patagium (gliding membrane). Scale bar, 20 mm. **b**–**e**, Bones as rendered from computed tomography scans. **b**, Cranium in right oblique dorsal view, right mandible in lateral view and left mandible in medial view. Scale bars, 1 mm (**d**, **e**), 2 mm (**c**), 5 mm (**b**). **c**, Left mandible in medial view, showing the disposition of the auditory elements and the absence of postdentary trough and Meckelian sulcus. **d**, Left incus (blue) in ventral view, left malleus (green) in dorsal view and left ectotympanic (red) in ventral view. **e**, Left incus, malleus and ectotympanic restored to life position in oblique dorsal and ventral views (right and left, respectively). Colours for the auditory elements are as in Fig. 1. al, anterior limb of ectotympanic; an, angular process; api, anterior prominence of incus; apm, anterior process of malleus; cb, crus breve; co, mandibular condyle; cp, coronoid process; e, ectotympanic; fapm, facet for anterior process of malleus; fe, facet for ectotympanic; fi, facet for incus; fma, facet for malleus; fr, frontal; ju, jugal; lac, lacrimal; li, left incus; lm, left mandible; lma, left malleus; mab, mallear body; mas, mandibular symphysis; mf, mandibular foramen; mm, manubrium of malleus; mx, maxilla; na, nasal; pa, parietal; pal, palatine; pl, posterior limb of ectotympanic; pmx, premaxilla; ptf, pterygoid fossa; ri, right incus; rl, reflected lamina of ectotympanic; rm, right mandible; rma, right malleus; smx, septomaxilla; sp, stapedial process; sq, squamosal; ts, tympanic sulcus.

Middle-to-Late Jurassic epochs of England[23,24] and Siberia[25], Late Jurassic epoch of China[26], and Early Cretaceous epoch of Siberia[27] (Extended Data Figs. 7, 8, Supplementary Information). The haramiyidan clade is in a polytomy with *Cifelliodon* from the Early Cretaceous epoch of North America[16] and Multituberculata + Gondwanatheria, as recently supported[28]. These lineages are included in Allotheria, which also includes *Haramiyavia* from the Late Triassic epoch of Greenland[18]. Allotheria is included in Mammalia, which supports a 'long fuse' model in which crown mammals originated at least 215 million years ago[29]. However, in our Bayesian analysis (Extended Data Fig. 9) Allotheria is in a polytomy that includes the monotreme and therian lineages.

Evolution of the mammalian middle ear

Our phylogenies have several implications for understanding the evolution of the auditory apparatus. As noted above, the three types of middle ear can be differentiated on the basis of the morphology of the medial surface of the lower jaw (Fig. 1); however, elucidating the details of the auditory apparatus in these three types requires the auditory bones to be preserved. Of the 106 extinct taxa in our phylogenetic analysis, 76% can be scored for the postdentary trough and Meckelian sulcus. By contrast, only 17% of the extinct taxa can be scored for features of the incus (quadrate). We are therefore more confident in differentiating the three types of middle ear than we are in elucidating the transformations of the auditory elements between these types.

Our phylogenetic trees relate a complex history of the postdentary trough and Meckelian sulcus, which supports several independent detachments of the postdentary bones. Optimized in the strict consensus tree from the maximum parsimony analysis (Extended Data Fig. 8), the postdentary trough is lost twice independently in mammals (within Austalosphenida and in Boreosphenida, with a reacquisition in *Haramiyavia*), whereas the Meckelian sulcus is lost eight times independently (twice within Australosphenida, in the Middle Jurassic *Volaticotherium*, within Allotheria, in the Early Cretaceous *Vincelestes*, twice within Eutheria and in Metatheria, with a reacquisition in *Kokopellia*). It is generally held that a Meckelian sulcus has a Meckel's cartilage within it[30,31] and—in turn—that Meckel's cartilage has continuity with the malleus, given the embryonic origin of the latter from the former[32]. However, the presence of the sulcus does not mandate continuity between Meckel's cartilage and the malleus, as the sulcus persists (for example) in a neonatal African palm civet well after the isolation of the malleus[33]. A recent report on the middle ear of the Early Cretaceous zhangheotheriid *Origolestes*[6] described an ossified Meckel's cartilage in the Meckelian sulcus that is separated from the malleus by a narrow gap (Fig. 3g), which was accepted as real and used to reconstruct a detached middle ear[6]. This is a possible interpretation, but the authors[6] noted 'In all specimens we have, the ossified Meckel's cartilage has been displaced at various degrees, which suggests that the ossified Meckel's cartilage was held by soft tissue to the Meckelian groove in life and easily displaced in preservation'. It seems possible that
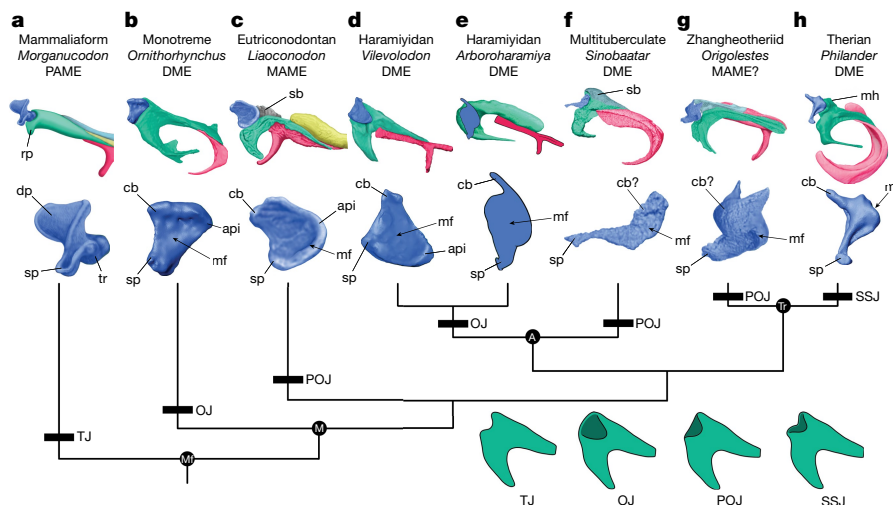
Article

Fig. 3 | The incudomallear articulation across Mammaliaformes.
a–h, Auditory apparatuses in medial (**a**, **c**, **g**, **h**) or dorsal (**b**, **d**–**f**) views. **a**, *Morganucodon*[13,45]. **b**, *Ornithorhynchus anatinus* (Carnegie Museum 50815). **c**, *Liaoconodon hui*[6,14,22]. **d**, *Vilevolodon diplomylos* (IMMNH-PV01699). **e**, *Arboroharamyia allinhopsoni* (see Supplementary Information for the basis of our reinterpretation of refs. [3,17]). **f**, *Sinobaatar pani*[22]. **g**, *Origoletes lii*[6,22]. **h**, *Philander opossum* (Carnegie Museum 110578). We identify four types of incudomallear joint, as indicated on the malleus (articular) with articular facet in dark green: trochlear joint (TJ) (in nonmammalian cynodonts), overlapping joint (OJ), partial overlapping joint (POJ) and saddle-shaped joint (SSJ) (in therians). Black bars indicate the presence of these types of joint in the simplified consensus tree of our parsimony analysis (Extended Data Fig. 7). The characters from our phylogenetic analysis (Supplementary Information,

characters 415–419) associated with the overlapping joint optimize as primitive for Mammalia. Auditory ossicles are unknown in early members of Allotheria and Australosphenida (which includes monotremes), with their mandibles indicating a postdentary-attached middle ear (PAME); their incus (quadrate) may have been more weight-bearing (as in nonmammalian cynodonts), in which case the overlapping joint may have evolved convergently in these lineages. Colours for the auditory elements are as in Fig. 1. In **b**–**g**, the arrows labelled 'mf' indicate a malleus facet on the concealed surface of the incus. A, Allotheria; DME, detached middle ear; dp, dorsal plate; M, Mammalia; MAME, Meckelian-attached middle ear; Mf, Mammaliaformes; mf, malleus facet; mh, malleus head; rp, retroarticular process; sb, surangular boss; Tr, Trechnotheria; tr, trochlea. Not to scale.

such displacement could separate the ossified Meckel's element from the auditory apparatus, which means that the gap may be an artefact of preservation and the middle ear may be of the Meckelian-attached type.

Among extant mammals, the morphology of the incus of *Vilevolodon* and its articulation with the malleus closely matches that of monotremes (Fig. 3b, d). Both the platypus and echidna have a flat, triangular incus with short stapedial process and crus breve, and an anterior prominence; the incus is tightly bound to the malleus by dense connective tissue and cartilage[34,35]. In situ, the monotreme incus lies dorsal to the malleus with a relatively flat articulation between them (which we term an overlapping joint) (Fig. 3), and the tympanic membrane is roughly horizontal (Extended Data Fig. 5d). Given the notable similarities to the monotreme ossicles, we suggest *Vilevolodon* also had an incus dorsal to—and with little movement on—the malleus, and a roughly horizontal tympanic membrane. The arrangement of the incus and malleus in monotremes (and *Vilevolodon*) is unlike that in extant therians, in which the incus generally lies caudal to the malleus, has a distinct body with complex concavoconvex or saddle-shaped articular surfaces that contact reciprocally complex articular surfaces on the malleus, and an elongate stapedial process and crus breve[34,36] (Fig. 3h); the therian tympanic membrane is usually oblique or vertical.

Among extinct mammals, details of the morphology of the incus and its articulation with the malleus are limited to a handful of Mesozoic mammals, most of which have been reported in the past few years. The overlapping incudomallear articulation in *Vilevolodon* resembles that described for the haramiyidan *A. allinhopsoni*[3,17] (Fig. 3d, e) and the Early Cretaceous multituberculate *Jeholbaatar*[5] and eutriconodontan *Yanoconodon*[37]. However, in *Jeholbaatar*, the element identified as the incus[5] is now interpreted to be part of the malleus on the basis of the morphology of another Early Cretaceous multituberculate (*Sinobaatar pani*)[22], and—in *Yanoconodon*—photographic or computed tomography documentation of an overlapping articulation has not yet been provided[37]. Consequently, we treat the incudomallear articulation as

unknown in *Jeholbaatar* and *Yanoconodon*. The morphology of the incus of *Vilevolodon* is similar to that of the Early Cretaceous eutriconodontan *Liaoconodon*[6,14,22] (Fig. 3c, d), which has a Meckelian-attached middle ear (Fig. 1b); in both, the incus is flat with a triangular outline, short stapedial process and crus breve, and a gently convex mallear articular surface. The major difference between the incus morphology of these taxa is the degree of overlap with the malleus; the incus in *Vilevolodon* fully overlaps the malleus but the overlap is only partial in *Liaoconodon*, limited to the anterior prominence (Fig. 3 and supplementary movie 5 of ref. [22]). Another difference is the reconstructed angulation of the tympanic membrane as horizontal in *Vilevolodon* and vertical in *Liaoconodon*[6,22]. A partial overlapping joint (also known as braced hinge joint)[22] also occurs in *S. pani* (Fig. 3f) and *Origolestes*[22] (Fig. 3g); however, both differ from *Liaoconodon* in having a long stapedial process and, in addition, *Origolestes* has a thickened incudal body.

The partial overlapping joint has recently been proposed as primitive for Mammalia, easily derivable from the trochlear joint (quadroarticular) of nonmammalian cynodonts[22]. The partial overlapping joint is hypothesized to be the precursor of both the overlapping and saddle-shaped joints, by a dorsal shift of the incus in the former and a caudal shift of the incus in the latter[22]. In contrast to this model, optimization of the five characters of the incudomallear joint (characters 415–419 in Supplementary Information) in the consensus tree of our parsimony analysis supports the overlapping joint as primitive for Mammalia (Fig. 3). The partial overlapping joint is derived from the overlapping joint (and not vice versa) by the caudal shift of the incus with regard to the malleus (Fig. 3). The ontogeny of extant therians reflects this direction for the transformation of the incudomallear joint. A monotreme-like overlapping incudomallear condition appears first in therian ontogeny (Extended Data Fig. 10a, Supplementary Information), with the main mass of the incus dorsal to the malleus and a more planar joint in marsupial pouch-young[38,39] and placental embryos[40,41]. Moreover, on early ontogenetic appearance in monotremes and some

marsupials and placentals, the incus has a broader abutment or fusion with the petrosal bone than in the adult[42,43], which in the case of hatchling monotremes and marsupial pouch-young is able to function substantially before the temporomandibular jaw joint does[43].

Fossil mammals leading to the haramiyidan and monotreme lineages—early members of Allotheria[44] and Australosphenida[13], respectively—had postdentary-attached middle ears. As the incus and malleus are not known in these early allotherians and australosphenidans, this middle ear reconstruction is indicated by the presence of a postdentary trough and Meckelian sulcus (Fig. 1a). Fossils with a postdentary-attached middle ear in which the incus (quadrate) is preserved (for example, *Morganucodon*[45]) have a morphology for that element unlike that in either Meckelian-attached or detached middle ears (Fig. 3a). The quadrate in postdentary-attached middle ears is more of a weight-bearing structure and has a rostrocaudal contact with the malleus (articular) via a convex, cylindrical trochlea and a robust dorsal plate that broadly contacts the petrosal bone (Fig. 3a). It is uncertain whether early allotherians and australosphenidans with a postdentary-attached middle ear had a similar weight-bearing incus and, therefore, whether the overlapping articulation present in monotremes and Tiaojishan haramiyidans evolved convergently, or whether the overlapping joint represents a shared innovation at the level of Mammalia. Perhaps, during detachment of the postdentary bones, the overlapping joint balanced the needs both for increased auditory acuity and for load-bearing through a small crus breve and incudomallear joint with little movement. No matter which evolutionary trajectory occurred, the specimen of *Vilevolodon* reported here clarifies the morphology of the auditory apparatus in haramiyidans and shows that monotremes are not unique in their auditory apparatus, as has previously been proposed[22,34,45,46], and that several long-lived mammalian lineages co-opted similar incudal morphologies.

Online content

Any methods, additional references, Nature Research reporting summaries, source data, extended data, supplementary information, acknowledgements, peer review information; details of author contributions and competing interests; and statements of data and code availability are available at https://doi.org/10.1038/s41586-020-03137-z.

1. Manley, G. A. & Sienknecht, U. J. in *The Middle Ear: Science, Otosurgery and Technology* (eds Puria, S. et al.) 7–30 (Springer, 2013).
2. Allin, E. F. & Hopson, J. A. in *The Evolutionary Biology of Hearing* (eds Webster, D. B. et al.) 587–614 (Springer, 1992).
3. Han, G., Mao, F., Bi, S., Wang, Y. & Meng, J. A Jurassic gliding euharamiyidan mammal with an ear of five auditory bones. *Nature* **551**, 451–456 (2017).
4. Luo, Z.-X. et al. New evidence for mammaliaform ear evolution and feeding adaptation in a Jurassic ecosystem. *Nature* **548**, 326–329 (2017).
5. Wang, H., Meng, J. & Wang, Y. Cretaceous fossil reveals a new pattern in mammalian middle ear evolution. *Nature* **576**, 102–105 (2019).
6. Mao, F. et al. Integrated hearing and chewing modules decoupled in a Cretaceous stem therian mammal. *Science* **367**, 305–308 (2020).
7. Luo, Z.-X. Transformation and diversification in early mammal evolution. *Nature* **450**, 1011–1019 (2007).
8. Meng, J. Mesozoic mammals of China: implications for phylogeny and early evolution of mammals. *Natl Sci. Rev.* **1**, 521–542 (2014).
9. Zheng, X., Bi, S., Wang, X. & Meng, J. A new arboreal haramiyid shows the diversity of crown mammals in the Jurassic period. *Nature* **500**, 199–202 (2013).
10. Bi, S., Wang, Y., Guan, J., Sheng, X. & Meng, J. Three new Jurassic euharamiyidan species reinforce early divergence of mammals. *Nature* **514**, 579–584 (2014).
11. Meng, Q. J. et al. New gliding mammaliaforms from the Jurassic. *Nature* **548**, 291–296 (2017).
12. Mao, F. Y. & Meng, J. A new haramiyidan mammal from the Jurassic Yanliao Biota and comparisons with other haramiyidans. *Zool. J. Linn. Soc.* **186**, 529–552 (2019).
13. Luo, Z.-X. Developmental patterns in Mesozoic evolution of mammal ears. *Annu. Rev. Ecol. Evol. Syst.* **42**, 355–380 (2011).
14. Meng, J., Wang, Y. & Li, C. Transitional mammalian middle ear from a new Cretaceous Jehol euriconodont. *Nature* **472**, 181–185 (2011).
15. Harper, T. & Rougier, G. W. Petrosal morphology and cochlear function in Mesozoic stem therians. *PLoS ONE* **14**, e0209457 (2019).
16. Huttenlocker, A. K., Grossnickle, D. M., Kirkland, J. I., Schultz, J. A. & Luo, Z.-X. Late-surviving stem mammal links the lowermost Cretaceous of North America and Gondwana. *Nature* **558**, 108–112 (2018).
17. Meng, J. et al. A comparative study on auditory and hyoid bones of Jurassic euharamiyidans and contrasting evidence for mammalian middle ear evolution. *J. Anat.* **236**, 50–71 (2020).
18. Jenkins, F. A. Jr, Gatesy, S. M., Shubin, N. H. & Amaral, W. W. Haramiyids and Triassic mammalian evolution. *Nature* **385**, 715–718 (1997).
19. Hahn, G. Neue Zähne von Haramiyiden aus der deutschen Ober-Trias und ihre Beziehungen zu den Multituberculaten. *Palaeontographica Abt. A Paläozool. Stratigr.* **142**, 1–15 (1973).
20. Meng, J., Bi, S., Zheng, X. & Wang, X. Ear ossicle morphology of the Jurassic euharamiyidan *Arboroharamiya* and evolution of mammalian middle ear. *J. Morphol.* **279**, 441–457 (2018).
21. Kermack, K. A., Mussett, F. & Rigney, H. W. The lower jaw of *Morganucodon*. *Zool. J. Linn. Soc.* **53**, 87–175 (1973).
22. Mao, F., Liu, C., Chase, M. H., Smith, A. K. & Meng, J. Exploring ancestral phenotypes and evolutionary development of the mammalian middle ear based on Early Cretaceous Jehol mammals. *Natl Sci. Rev.* https://doi.org/10.1093/nsr/nwaa188 (2020).
23. Kermack, K. A., Kermack, D. M., Lees, P. M. & Mills, J. R. E. New multituberculate-like teeth from the Middle Jurassic of England. *Acta Palaeontol. Pol.* **43**, 581–606 (1998).
24. Butler, P. M. & Hooker, J. R. New teeth of allotherian mammals from the English Bathonian, including the earliest multituberculates. *Acta Palaeontol. Pol.* **50**, 185–207 (2005).
25. Averianov, A. O. et al. Haramiyidan mammals from the Middle Jurassic of western Siberia, Russia. Part 1: Shenshouidae and *Maiopatagium*. *J. Vertebr. Paleontol.* **39**, e1669159 (2019).
26. Martin, T., Averianov, A. O. & Pfretzschner, H. U. Mammals from the Late Jurassic Qigu Formation in the southern Junggar Basin, Xinjiang, northwest China. *Palaeobio. Palaeoenv.* **90**, 295–319 (2010).
27. Averianov, A. O. et al. A new euharamiyidan mammaliaform from the Lower Cretaceous of Yakutia, Russia. *J. Vertebr. Paleontol.* **39**, e1762089 (2020).
28. Krause, D. W. et al. Skeleton of a Cretaceous mammal from Madagascar reflects long-term insularity. *Nature* **581**, 421–427 (2020).
29. Cifelli, R. L. & Davis, B. M. Jurassic fossils and mammalian antiquity. *Nature* **500**, 160–161 (2013).
30. Bensley, B. A. On the identification of Meckelian and mylohyoid grooves in the jaws of Mesozoic and recent Mammalia. *Univ. Tor. Stud. Biol. Ser.* **3**, 75–81 (1902).
31. Simpson, G. G. Mesozoic Mammalia. XII. The internal mandibular groove in Jurassic mammals. *Am. J. Sci.* **14**, 461–470 (1928).
32. Burford, C. M. & Mason, M. J. Early development of the malleus and incus in humans. *J. Anat.* **229**, 857–870 (2016).
33. Wible, J. R. & Spaulding, M. On the cranial osteology of the African palm civet, *Nandinia binotata* (Gray, 1830) (Mammalia, Carnivora, Feliformia). *Ann. Carnegie Mus.* **82**, 1–114 (2013).
34. Fleischer, G. Studien am Skelett des Gehörorgans der Säugetiere, einschließlich des Menschen. *Saugetierkdl. Mitt.* **21**, 131–239 (1973).
35. Zeller, U. in *Mammal Phylogeny: Mesozoic Differentiation, Multituberculates, Monotremes, Early Therians, and Marsupials* (eds Szalay, F. S. et al.) 95–107 (Springer, 1993).
36. Doran, A. H. G. Morphology of the mammalian ossicula auditûs. *Trans. Linnean Soc. Lond. 2nd Ser. Zool.* **1**, 371–497 (1878).
37. Luo, Z.-X., Chen, P., Li, G. & Chen, M. A new euticonodont mammal and evolutionary development in early mammals. *Nature* **446**, 288–293 (2007).
38. McClain, J. A. The development of the auditory ossicles of the opossum (*Didelphys virgininia*). *J. Morphol.* **64**, 211–265 (1939).
39. Sánchez-Villagra, M. R., Gemballa, S., Nummela, S., Smith, K. K. & Maier, W. Ontogenetic and phylogenetic transformations of the ear ossicles in marsupial mammals. *J. Morphol.* **251**, 219–238 (2002).
40. Anson, B. J., Hanson, J. S. & Richany, S. F. Early embryology of the auditory ossicles and associated structures in relation to certain anomalies observed clinically. *Ann. Otol. Rhinol. Laryngol.* **69**, 427–447 (1960).
41. Whyte, J. R. et al. Fetal development of the human tympanic ossicular chain articulations. *Cells Tissues Organs* **171**, 241–249 (2002).
42. Rodríguez-Vázquez, J. F., Yamamoto, M., Abe, S., Katori, Y. & Murakami, G. Development of the human incus with special reference to the detachment from the chondrocranium to be transferred into the middle ear. *Anat. Rec. (Hoboken)* **301**, 1405–1415 (2018).
43. Anthwal, N., Fenelon, J. C., Johnston, S. D., Renfree, M. B. & Tucker, A. S. Transient role of the middle ear as a lower jaw support across mammals. *eLife* **9**, e57860 (2020).
44. Luo, Z.-X., Gatesy, S. M., Jenkins, F. A., Jr, Amaral, W. W. & Shubin, N. H. Mandibular and dental characteristics of Late Triassic mammaliaform *Haramiyavia* and their ramifications for basal mammal evolution. *Proc. Natl Acad. Sci. USA* **112**, E7101–E7109 (2015).
45. Luo, Z. & Crompton, A. W. Transformation of the quadrate (incus) through the transition from non-mammalian cynodonts to mammals. *J. Vertebr. Paleontol.* **14**, 341–374 (1994).
46. Rougier, G. W., Wible, J. R. & Novacek, M. J. Middle-ear ossicles of the multituberculate *Kryptobaatar* from the Mongolian Late Cretaceous: implications for the mammaliamorph relationships and the evolution of the auditory apparatus. *Am. Mus. Novit.* **3187**, 1–43 (1996).

Article

Methods

Ethics oversight
Research design and process followed the ethics guidelines of Carnegie Museum of Natural History and Indiana University of Pennsylvania.

Computed tomography scanning
The main part and counterpart were scanned using a three-dimensional X-ray microscope, Zeiss Xradia 520 Versa at the Micro-CT Laboratory of Nanjing Institute of Geology and Palaeontology, Chinese Academy of Sciences (NIGPAS). The scanning had the following parameters: voltage of 90 kV, current of 88 μA and voxel size of 0.032707. The three-dimensional reconstructions were created with the software Mimics (version 16.1) and Amira-Avizo 2020.2.

Phylogenetic analysis
The data matrix consisting of 130 taxa and 509 characters was analysed using maximum parsimony and Bayesian inference. Parsimony analysis was performed in TNT[47] using a new technology search (sectorial search, ratchet, drift and tree fusing) set to 100 iterations, followed by a traditional search. All characters are unweighted and nonadditive. The search procedure resulted in 30 most-parsimonious trees of length 2,770 (consistency index = 0.311; retention index = 0.795). The strict consensus tree (2,871 steps; consistency index = 0.300; retention index = 0.784) of these 30 most-parsimonious trees is presented in Extended Data Fig. 8.

Tip-dating Bayesian analysis was performed in MrBayes 3.2.7[48] and run using Cyber Infrastructure for Phylogenetic Research[49]. To root the tree, we applied two topological constraints on the stem. For the likelihood model, we used a gamma-rate distribution and eight discrete rate categories to accommodate among character evolutionary-rate variation[50–53].

The fossilized birth–death process[54–57] was used to form a prior probability distribution on the space of sampled-ancestor trees through the modelling of speciation, extinction, fossilization and sampling. The age of each fossil taxon was assigned a uniform prior with upper and lower bounds that corresponded to a stage-level stratigraphic range. Fossil occurrences were taken from the literature or from the Fossilworks Paleobiology Database and recorded by stratigraphic stage using the International Chronostratigraphy chart[58]. The root age of the tree was assigned an offset exponential prior with a mean of 251 million years ago determined by the lower age range of the oldest fossil taxon (*Thrinaxodon*) and a minimum of 228 million years ago, corresponding to the beginning of the geological stage containing the first appearance of the next oldest fossil taxon (*Massetognathus*). For inference, we assigned defuse priors parameterizing the speciation, extinction and sampling rates. We used an exponential (100) prior for net diversification and beta distributions (1,1) for turnover and fossil sampling proportions. The sampling proportion of extant taxa (26 species) was set to 0.004, on the basis of the number of recognized living mammal species (6,495[59]). We calculated a clock rate using APE[60] and fitdistrplus[61] in R[62] and applied a data-informed clock rate prior using a previously published method[63] in R[62], which indicated the best model according to Bayesian information criterion was probably a normal distribution with a mean of 0.00840185218218286 and a s.d. of 0.0130196175801974. This model and its parameter values were used directly for the clock rate prior.

The posterior distribution was estimated using Markov chain Monte Carlo algorithms. The analysis was executed with 2 runs, each with 4 chains (1 cold and 3 hot) per run for 10 million iterations and sampled every 1,000 iterations. The first 25% samples were discarded as burn-in for each run, and the remaining samples from the 2 runs were combined after checking convergence between runs (average s.d. of the split frequencies < 0.05[64]). Runs were viewed in Tracer[65] to ensure stationarity was achieved. The dated phylogeny (Extended Data Fig. 9) was estimated from the 50% majority rule consensus of the pooled post burn-in trees. Posterior probabilities were calculated to assess node robustness and posterior medians provide node ages.

Reporting summary
Further information on research design is available in the Nature Research Reporting Summary linked to this paper.

Data availability
The specimen (IMMNH-PV01699) studied here has been deposited in the Inner Mongolia Museum of Natural History. The data matrix for the phylogenetic analysis is deposited in MorphoBank (project number 3760); computed tomography data are deposited in MorphoSource at https://doi.org/10.17602/M2/M167344.

Code availability
The Batch commands for the Bayesian analysis are included in the Supplementary Information.

47. Goloboff, P. A., Farris, J. S. & Nixon, K. C. TNT, a free program for phylogenetic analysis. *Cladistics* **24**, 774–786 (2008).
48. Huelsenbeck, J. P. & Ronquist, F. MRBAYES: Bayesian inference of phylogenetic trees. *Bioinformatics* **17**, 754–755 (2001).
49. Miller, M. A., Pfeiffer, W. & Schwartz, T. Creating the CIPRES Science Gateway for inference of large phylogenetic trees. In *2010 Gateway Computing Environments Workshop (GCE)* 1–8, https://doi.org/10.1109/GCE.2010.5676129 (IEEE, 2010).
50. Yang, Z. Maximum likelihood phylogenetic estimation from DNA sequences with variable rates over sites: approximate methods. *J. Mol. Evol.* **39**, 306–314 (1994).
51. Lewis, P. O. A likelihood approach to estimating phylogeny from discrete morphological character data. *Syst. Biol.* **50**, 913–925 (2001).
52. Wagner, P. J. Modelling rate distributions using character compatibility: implications for morphological evolution among fossil invertebrates. *Biol. Lett.* **8**, 143–146 (2012).
53. Harrison, L. B. & Larsson, H. C. E. Among-character rate variation distributions in phylogenetic analysis of discrete morphological characters. *Syst. Biol.* **64**, 307–324 (2015).
54. Stadler, T. Sampling-through-time in birth–death trees. *J. Theor. Biol.* **267**, 396–404 (2010).
55. Heath, T. A., Huelsenbeck, J. P. & Stadler, T. The fossilized birth–death process for coherent calibration of divergence-time estimates. *Proc. Natl Acad. Sci. USA* **111**, E2957–E2966 (2014).
56. Gavryushkina, A., Welch, D., Stadler, T. & Drummond, A. J. Bayesian inference of sampled ancestor trees for epidemiology and fossil calibration. *PLOS Comput. Biol.* **10**, e1003919 (2014).
57. Zhang, C., Stadler, T., Klopfstein, S., Heath, T. A. & Ronquist, F. Total-evidence dating under the fossilized birth–death process. *Syst. Biol.* **65**, 228–249 (2016).
58. Cohen, K. M., Finney, S. C., Gibbard, P. L. & Fan, J.-X. The ICS international chronostratigraphic chart. *Episodes* **36**, 199–204 (2013).
59. Burgin, C. J., Colella, J. P., Kahn, P. L. & Upham, N. S. How many species of mammals are there? *J. Mamm.* **99**, 1–34 (2018).
60. Paradis, E., Claude, J. & Strimmer, K. APE: analyses of phylogenetics and evolution in R language. *Bioinformatics* **20**, 289–290 (2004).
61. Delignette-Muller, M. L. & Dutang, C. fitdistrplus: an R package for fitting distributions. *J. Stat. Softw.* **64**, 1–34 (2004).
62. R Core Team. *R: A Language and Environment for Statistical Computing* (R Foundation for Statistical Computing, 2016).
63. Gunnell, G. F. et al. Fossil lemurs from Egypt and Kenya suggest an African origin for Madagascar's aye-aye. *Nat. Commun.* **9**, 3193 (2018).
64. Ronquist, F. et al. MrBayes 3.2: efficient Bayesian phylogenetic inference and model choice across a large model space. *Syst. Biol.* **61**, 539–542 (2012).
65. Rambaut, A., Drummond, A. J., Xie, D., Baele, G. & Suchard, M. A. Posterior summarization in Bayesian phylogenetics using Tracer 1.7. *Syst. Biol.* **67**, 901–904 (2018).
66. Hahn, G., Sigogneau-Russell, D. & Wouters, G. New data on Theroteinidae: their relations with Paulchoffatiidae and Haramiyidae. *Geol. Paleontol.* **23**, 205–215 (1989).
67. King, B. & Beck, R. M. D. Tip dating supports novel resolutions of controversial relationships among early mammals. *Proc. R. Soc. Lond. B* **287**, 20200943 (2020).
68. Gates, G. R., Saunders, J. C., Bock, G. R., Aitkin, L. M. & Elliott, M. A. Peripheral auditory function in the platypus, *Ornithorhynchus anatinus*. *J. Acoust. Soc. Am.* **56**, 152–156 (1974).
69. Sansom, R. S., Choate, P. G., Keating, J. N. & Randle, E. Parsimony, not Bayesian analysis, recovers more stratigraphically congruent phylogenetic trees. *Biol. Lett.* **14**, 20180263 (2018).
70. Hagenbach, E. Ueber ein besonderes, mit dem Hammer der Säugethiere in Verbindung stehendes Knöchelchen. *Arch. Anat. Physiol. Wissensch. Medizin* **1841**, 46–54 (1841).
71. Maier, W. & Ruf, I. The anterior process of the malleus in Cetartiodactyla. *J. Anat.* **228**, 313–323 (2016).

72. Broom, R. On the structure of the skull in *Chrysochloris*. *Proc. Zool. Soc. Lond.* **86**, 449–458 (1916).

Competing interests The authors declare no competing interests.

Additional information
Supplementary information The online version contains supplementary material available at https://doi.org/10.1038/s41586-020-03137-z.
Correspondence and requests for materials should be addressed to J.R.W. or S.B.
Peer review information *Nature* thanks Robin Beck, Simone Hoffmann and Guillermo Rougier for their contribution to the peer review of this work.
Reprints and permissions information is available at http://www.nature.com/reprints.
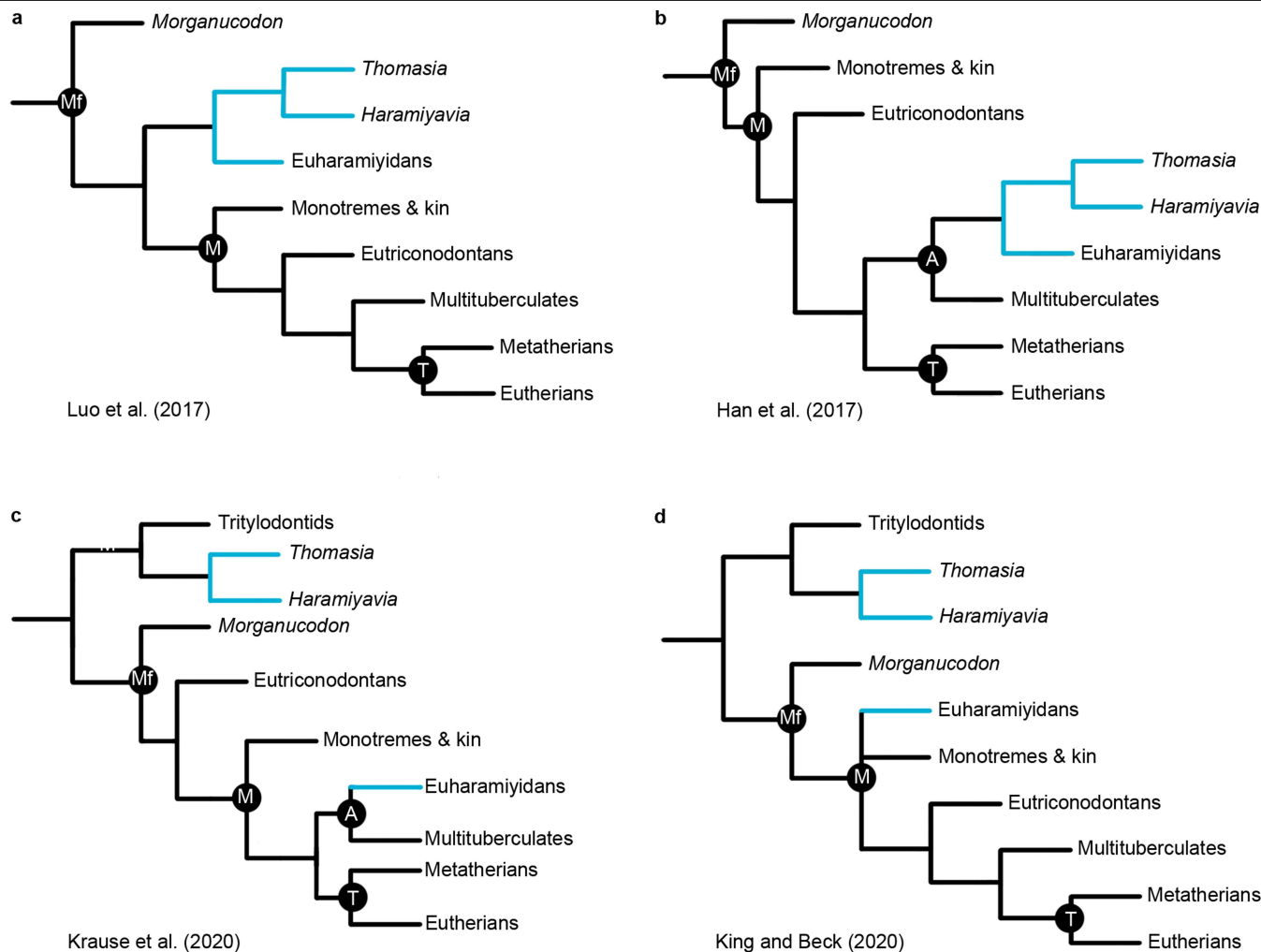
Extended Data Fig. 1 | Cladograms to illustrate various hypotheses regarding haramiyidan relationships. The Middle Jurassic Tiaojishan haramyidans are here included in Euharamiyida[10] (a junior synonym of Haramiyida[66] in our phylogenetic analysis (Supplementary Information)). Clades considered to be close relatives of euharamiyidans are in blue in each tree (simplified from the originals). **a**, Euharamiyidans are in a monophyletic Haramiyida, positioned outside of Mammalia (parsimony and Bayesian analyses in ref. [4]). **b**, Euharamiyidans are in a monophyletic Haramiyida, positioned within Mammalia in Allotheria with multituberculates; the gondwanatherian *Vintana* (not shown) is within Trechnotheria (parsimony and Bayesian analyses in ref. [3]). **c**, Haramiyidans are polyphyletic; euharamiyidans fall within Mammalia in Allotheria with multituberculates, and *Thomasia* and *Haramiyavia* form a clade with tritylodontids outside Mammaliaformes; gondwanatherians (not shown) are sister to multituberculates (parsimony analysis in ref. [28]). **d**, Haramiyidans are polyphyletic; euharamiyidans fall within Mammalia, and *Thomasia* and *Haramiyavia* form a clade with tritylodontids outside Mammaliaformes; the gondwanatherian *Vintana* (not shown) is within Euharamiyida (tip-dated Bayesian analysis in ref. [67]). A, Allotheria; M, Mammalia; Mf, Mammaliaformes; T, Theria.
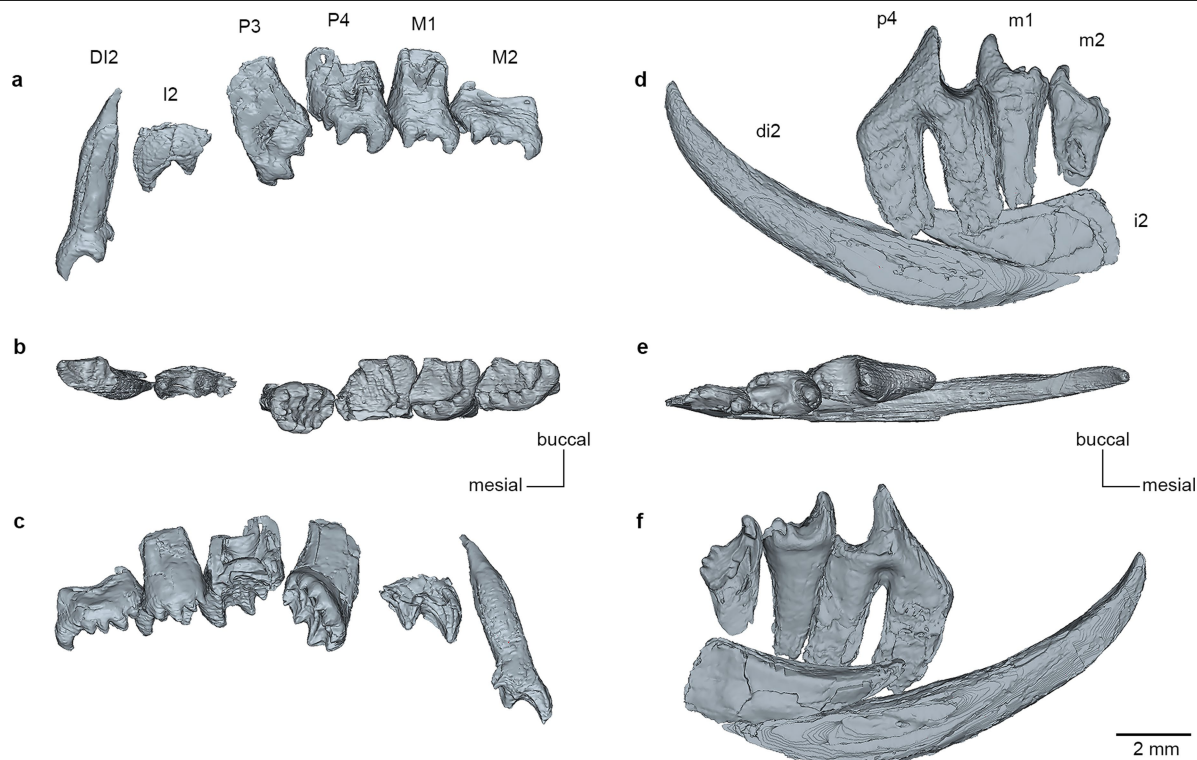
Extended Data Fig. 2 | Dentition of *V. diplomylos* (IMMNH-PV01699A). a–c, Upper left dentition in buccal (**a**), occlusal (**b**) and lingual (**c**) views. **d–f**, Lower left dentition in buccal (**d**), occlusal (**e**) and lingual (**f**) views. Regarding the numbering of the incisors, all haramiyidans for which the dentition is known have one upper and lower incisor (except for *Xianshou linglong* with two upper incisors[10]). The distal enlarged incisor was identified as I^2 with a tiny I^1 mesial to

it; the lower incisor was identified as i_2 as it occludes with upper I^2. DI^2, deciduous upper incisor; di_2, deciduous lower incisor; I^2, upper incisor; i_2, lower incisor; M^1, upper first molar; m_1, lower first molar; M^2, upper second molar; m_2, lower second molar; P^3, upper third premolar; P^4, upper fourth premolar; p_4, lower fourth premolar.
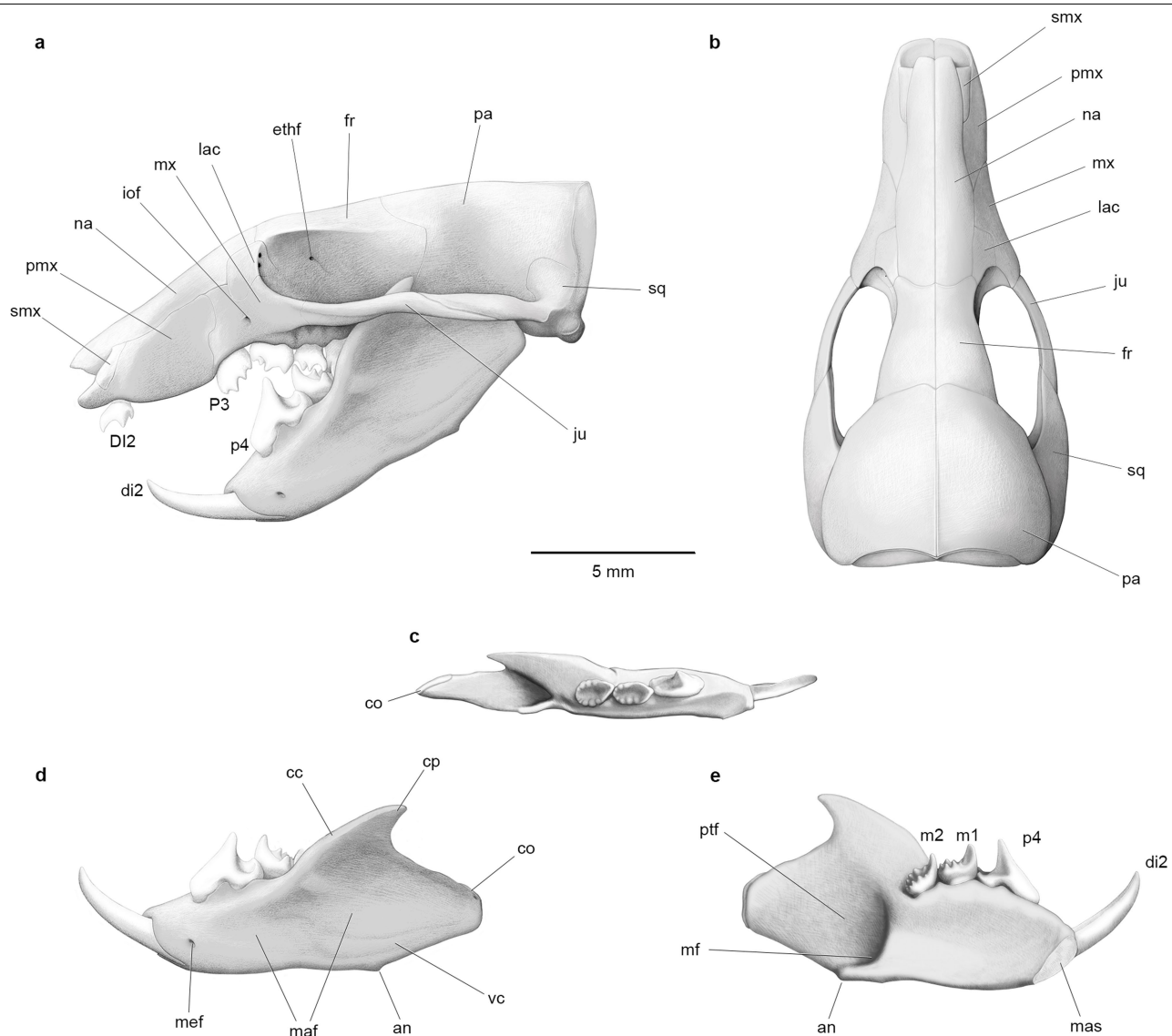
Extended Data Fig. 3 | Reconstruction of the skull of *V. diplomylos* (IMMNH-PV01699A and B). a, Skull in lateral view. **b**, Cranium in dorsal view. **c**–**e**, Left mandible in occlusal (**c**), lateral (**d**) and medial (**e**) views. an, angular process; cc, coronoid crest; co, mandibular condyle; cp, coronoid process; DI^2, deciduous upper incisor; di_2, deciduous lower incisor; ethf, ethmoidal foramen; fr, frontal; iof, infraorbital foramen; ju, jugal; lac, lacrimal; m_1, lower first molar; m_2, lower second molar; maf, masseteric fossa; mas, mandibular symphysis; mef, mental foramen; mf, mandibular foramen; mx, maxilla; na, nasal; P^3, upper third premolar; p_4, lower fourth premolar; pa, parietal; pmx, premaxilla; ptf, pterygoid fossa; smx, septomaxilla; sq, squamosal; vc, ventral crest.
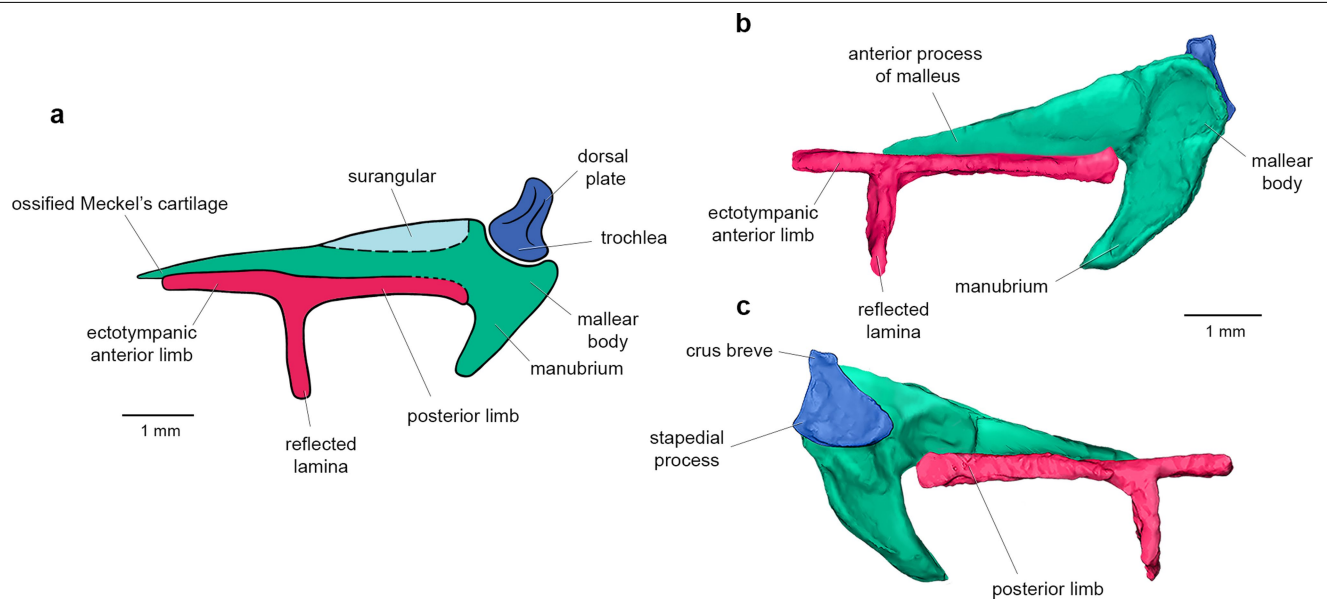
Extended Data Fig. 4 | Reconstructions of auditory apparatus in
***V. diplomylos* on the basis of the holotype versus the referred specimen. a**,
Reconstruction on the basis of the *Vilevolodon* holotype[4], which has
more-fragmentary auditory elements: the incus is shown with a trochlea and
dorsal plate (as in *Morganucodon*) (Fig. 3a) in a rostrocaudal incudomallear
articulation, and the malleus includes ossified Meckel's cartilage and

surangular. **b**, **c**, Reconstruction on the basis of the *Vilevolodon* referred
specimen (IMMNH-PV01699A) with well-preserved auditory elements in
ventral (**b**) and dorsal (**c**) views: the incus is flat and has a dorsoventral
incudomallear articulation, and the malleus does not have an ossified Meckel's
cartilage or surangular. Colours for the auditory elements are as in Fig. 1.
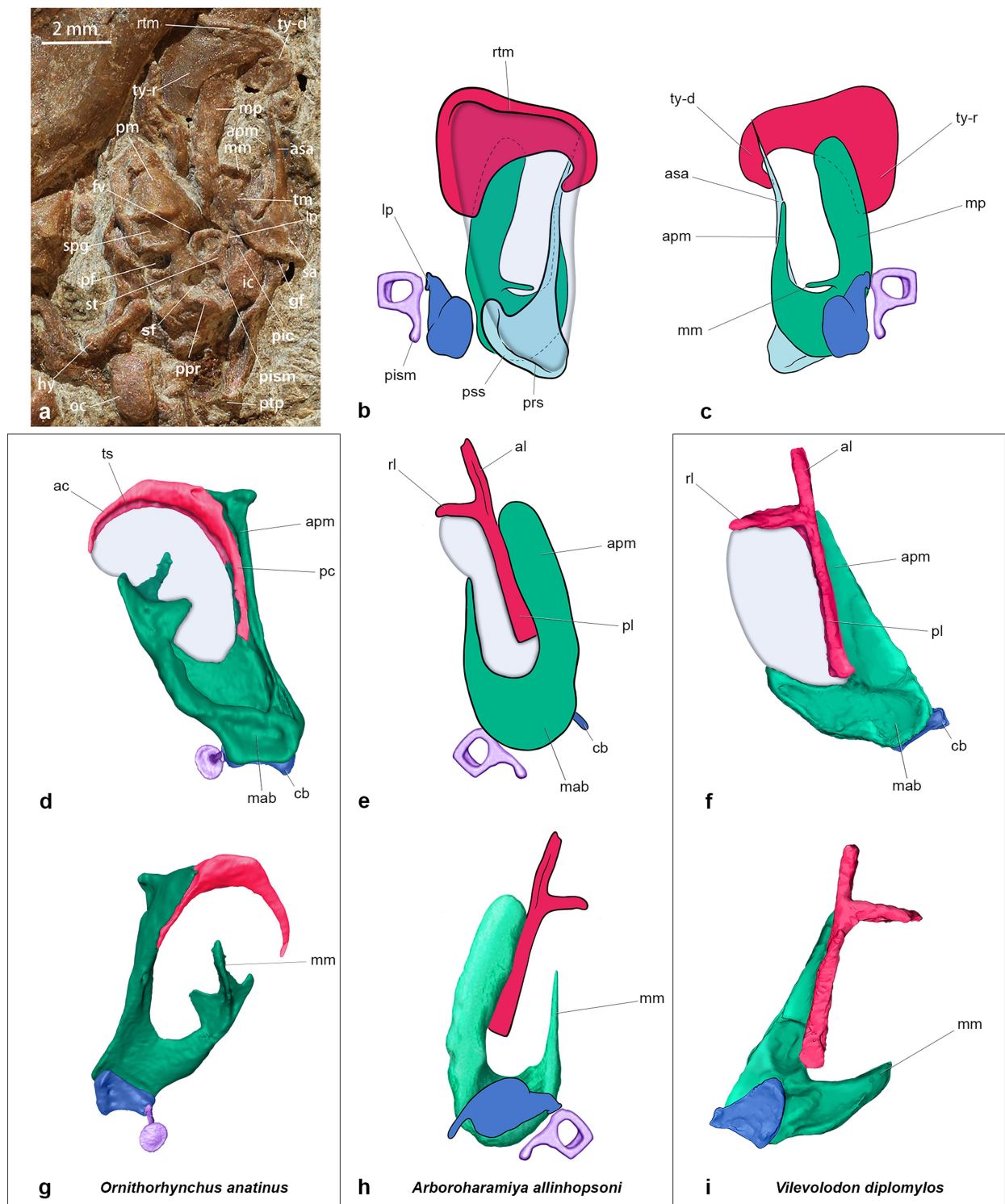
Extended Data Fig. 5 | See next page for caption.

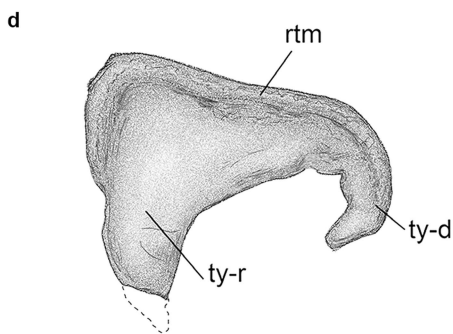**Extended Data Fig. 5 | Reinterpretation of auditory apparatus of *A. allinhopsoni*.** a–c, e, h, *Arboroharamiya allinhopsoni*, left auditory apparatus. a, Photograph of the holotype in ventral view (derived from extended data figure 5a of ref. [3]). b, c, Reconstruction in ventral (b) and dorsal (c) views (modified from extended data figure 5e, f of ref. [3]). e, h, The reconstruction proposed in this Article, in ventral (e) and dorsal (h) views (Supplementary Information). d, g, *Ornithorhynchus anatinus* (Carnegie Museum 50815), left auditory apparatus rendered from computed tomography scans in ventral (d) and dorsal (g) views. f, i, *Vilevolodon diplomylos* (IMMNH-PV01699A), left auditory apparatus in ventral (f) and dorsal (i) views. The crus breve of the incus in e and h is based on ref. [17]. Colours for the auditory elements are as in Fig. 1; stapes in purple; tympanic membrane (grey) is reconstructed on the ventral views in b, d[35,68], f. ac, anterior crus of ectotympanic; al, anterior limb of ectotympanic; apm, anterior process of malleus; asa, anterior process of surangular; cb, crus breve; fv, fenestra vestibuli; gf, glenoid fossa; hy, hyoid element; ic, incus; lp, lenticular process; mab, mallear body; mm, manubrium of malleus; mp, medial process of malleus; oc, occipital condyle; pc, posterior crus of ectotympanic; pf, perilymphatic foramen; pic, stapedial process of incus; pism, process for insertion of stapedius muscle of stapes; pl, posterior limb of ectotympanic; pm, promontorium; ppr, paroccipital process of petrosal; prs, posterior ridge of surangular; pss, posterior surface of surangular; ptp, posttympanic process of squamosal; rl, reflected lamina of ectotympanic; rtm, ridge for attachment for anterior part of tympanic membrane; sa, surangular; sf, stapedius fossa; spg, groove for stapedial artery; st, stapes; tm, transverse part of malleus; ts, tympanic sulcus; ty-d, lateral ectotympanic part presumably equivalent to dorsal part of angular; ty-r, ectotympanic part presumably equivalent to reflected lamina.
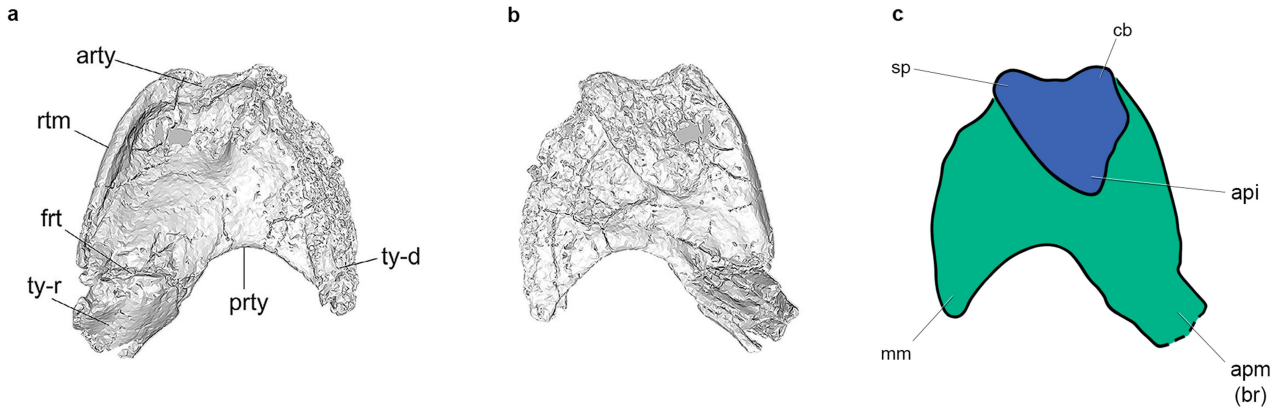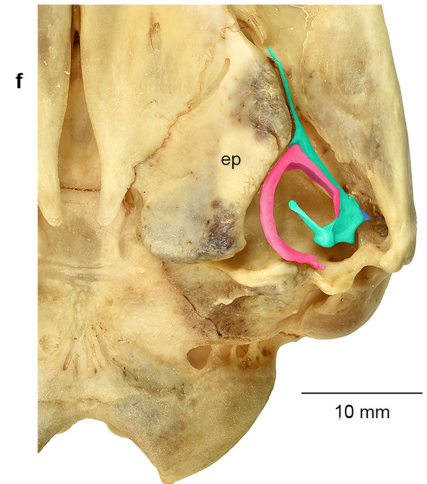
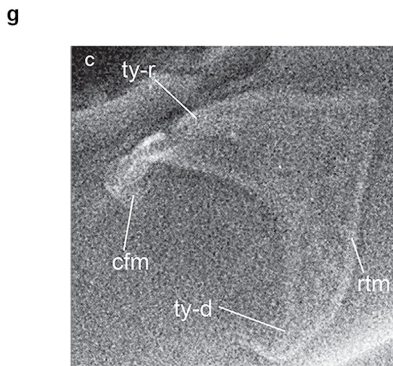**Extended Data Fig. 6 | Reinterpretation of ectotympanic of *Qishou* and *Arboroharamiya*. a–c**, *Qishou jintzang*, the so-called left ectotympanic in ventral (**a**) and dorsal (**b**) views, derived from figure 8c, d of ref. [17]; interpreted here as the left malleus with broken anterior process and incus in dorsal view (**c**). **d**, *Arboroharamiya allinhopsoni*, the so-called left ectotympanic in ventral view, derived from figure 3 of ref. [17]. **e**, **f**, *Tachyglossus aculeatus* (Carnegie Museum 50812), isolated left ectopterygoid bone and the left basicranium in ventral view. **g**, *Arboroharamiya jenkinsi*, the so-called left ectotytmpanic in ventral view, derived from figure 7c of ref. [17]. **h**, **i**, *Ornithorhynchus anatinus* (Carnegie Museum 50815), isolated left ectopterygoid bone and the left basicranium in ventral view. Colours for the auditory elements are as in Fig. 1. api, anterior prominence of incus; apm(br), anterior process of malleus (broken); arty, anterior edge of ectotympanic; cb, crus breve; cfm, contact area for malleus; ep, ectopterygoid; frt, fracture; mm, manubrium of malleus; prty, posterior edge of ectotympanic; rtm, ridge for attachment of anterior part of tympanic membrane; sp, stapedial process of incus; ty-d, lateral ectotympanic part presumably equivalent to dorsal part of angular; ty-r, ectotympanic part presumably equivalent to reflected lamina.
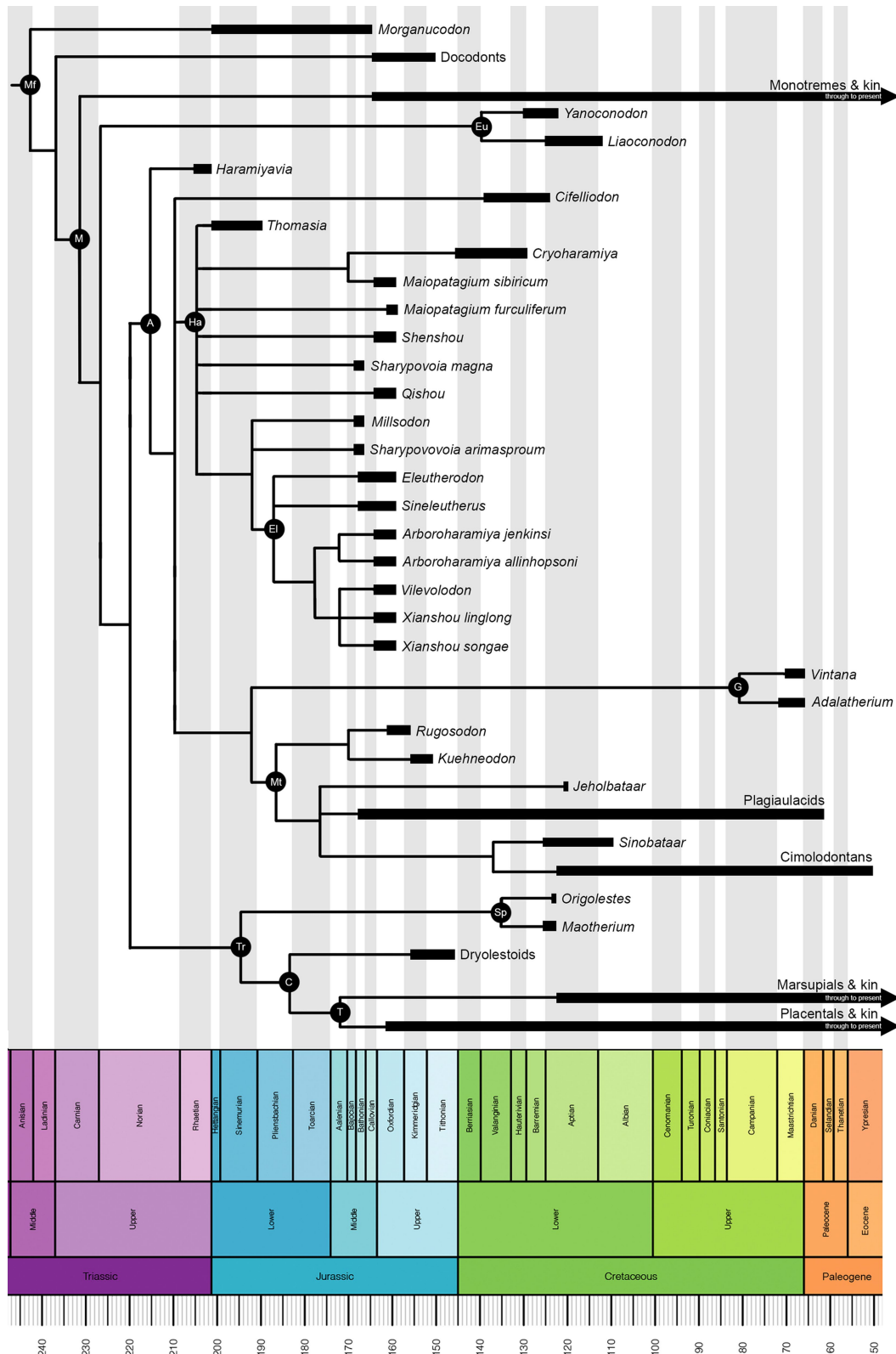
Extended Data Fig. 7 | Simplified strict-consensus parsimony tree, highlighting relationships and relative ages of key mammalian groups. The full tree is shown in Extended Data Fig. 8. Nodes are not time-calibrated. A,

Allotheria; C, Cladotheria; El, Eleutherodontidae; Eu, Eutriconodonta; G, Gondwanatheria; Ha, Haramiyida; M, Mammalia; Mf, Mammaliaformes; Mt, Multituberculata; Sp, Spalacotherioidea; T, Theria; Tr, Trechnotheria.
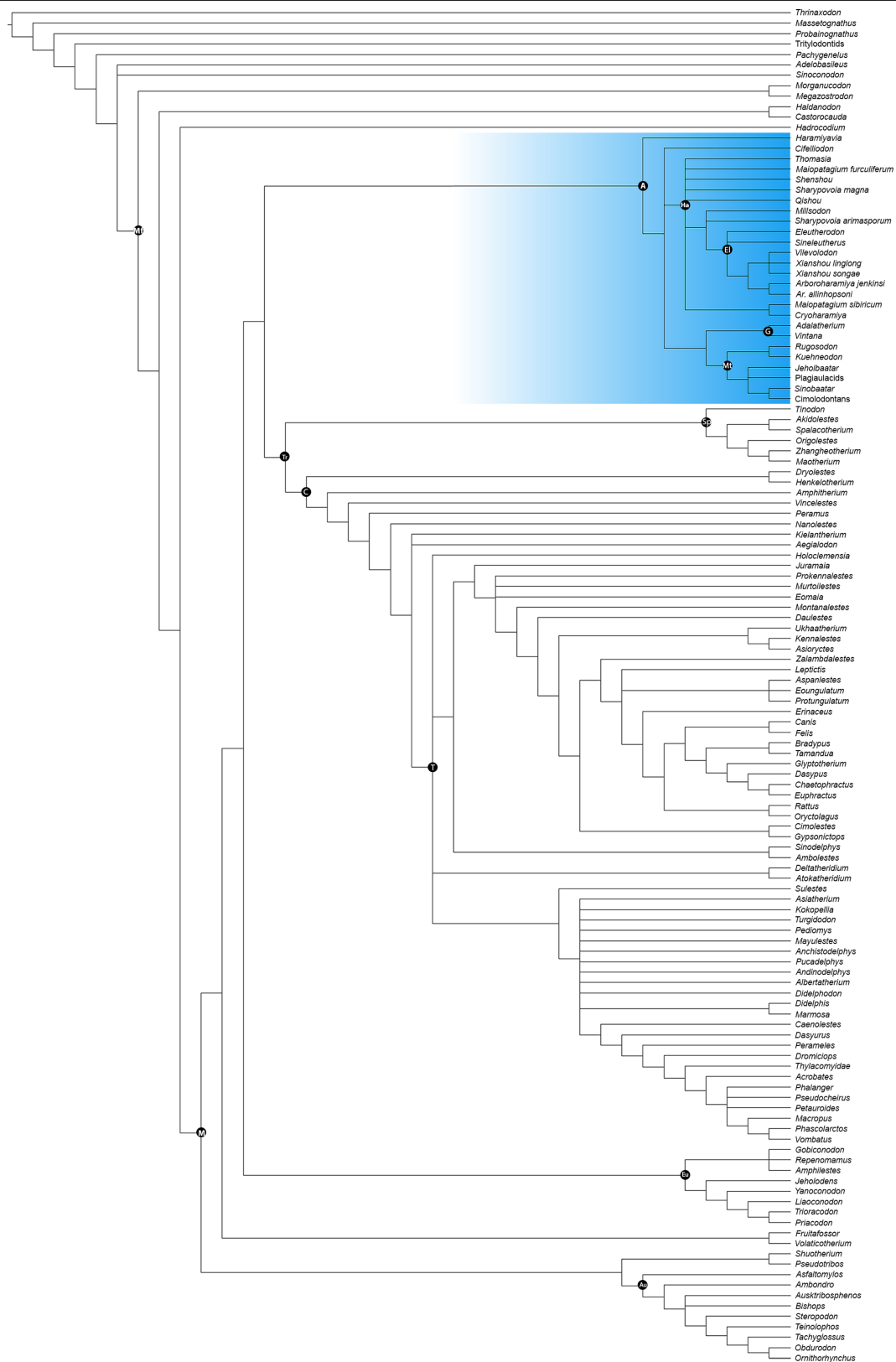
Extended Data Fig. 8 | Full parsimony consensus tree. The dataset comprises 130 taxa and 509 morphological characters. The strict consensus tree of 30 equally most-parsimonious trees was found in TNT[47]. Consensus tree length = 2,871; consistency index = 0.300; retention index = 0.784. The simplified version of this consensus tree is presented in Extended Data Fig. 7.

The allotherians (*Haramiyavia*, *Cifelliodon*, haramiyidans, multituberculates and gondwanatherians) are highlighted in blue. A, Allotheria; Au, Australosphenida; C, Cladotheria; El, Eleutherodontidae; Eu, Eutriconodonta; G, Gondwanatheria; Ha, Haramiyida; M, Mammalia; Mf, Mammaliaformes; Mt, Multituberculata; Sp, Spalacotherioidea; T, Theria; Tr, Trechnotheria.
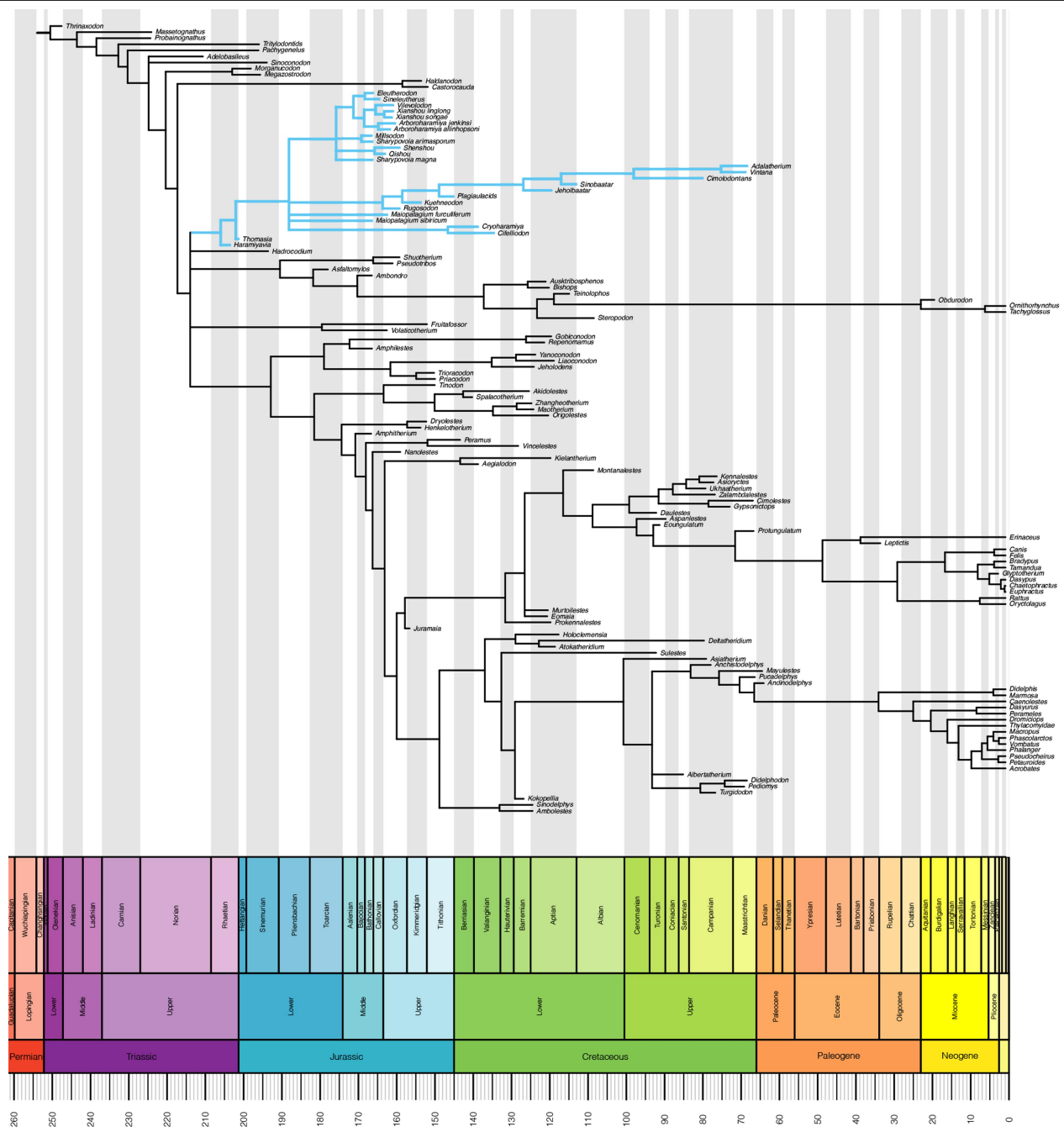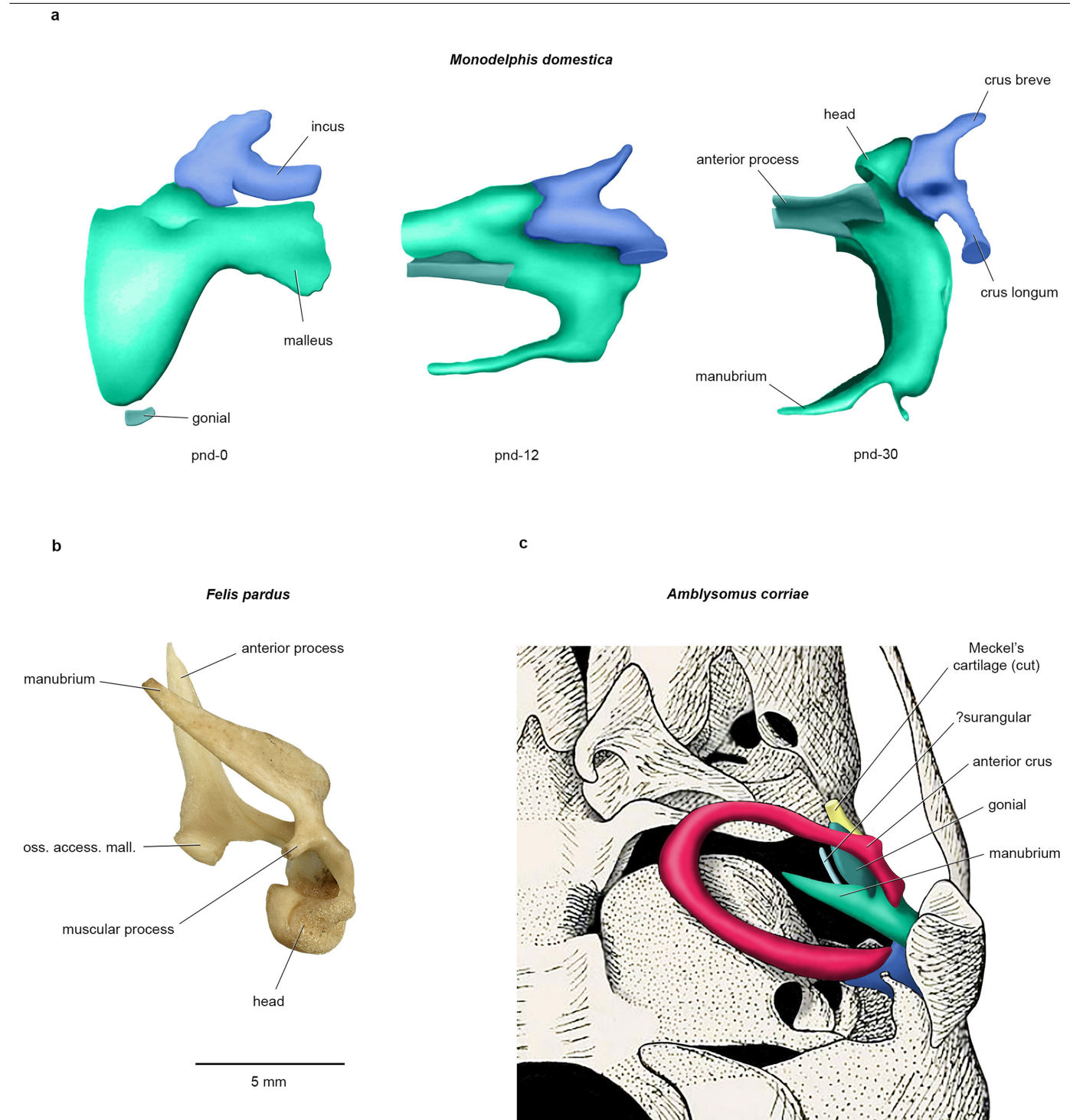
Extended Data Fig. 9 | Bayesian consensus tree. Fifty-per-cent majority rule consensus tree for Mesozoic mammals from a tip-dated analysis using Bayesian inference in MrBayes[64]. Tip-dating analysis confirms that mammals originated in the late Triassic (213.82 million years ago (207.98, 221.48 95% highest posterior density intervals)); however, the topology is different from the strict-consensus tree inferred from the parsimony analysis[69]. Allotherians are in blue.

a

Monodelphis domestica

pnd-0

pnd-12

pnd-30

b

Felis pardus

5 mm

c

Amblysomus corriae

Extended Data Fig. 10 | Ontogeny of auditory ossicles in extant therian mammals. a, Right malleus, incus and gonial on postnatal days 0, 12 and 30 of the didelphid marsupial *Monodelphis domestica* in medial view (redrawn from ref. [39]), anterior to the left and dorsal to the top. Incus is initially dorsal to the malleus and shifts caudally in later ontogenetic stages. **b**, Left malleus of the juvenile felid carnivoran *Felis pardus* (Carnegie Museum of Natural History (CM) 21006) in ventral view, medial to the left and anterior to the top, showing the ossiculum accessorium mallei[70] or processus internus praearticularis[71]. **c**, Left ear region of newborn golden mole *Amblysomus corriae* in ventral view, medial to the left and anterior to the top (modified from ref. [72]), showing the small, rod-like dermal element medial to the gonial that is posited to be the surangular. Colours for the ossicles are as in Fig. 1.

Corresponding author(s): John R. Wible and Shundong Bi

Last updated by author(s): Nov 22, 2020

Reporting Summary

Nature Research wishes to improve the reproducibility of the work that we publish. This form provides structure for consistency and transparency in reporting. For further information on Nature Research policies, see our Editorial Policies and the Editorial Policy Checklist.

Statistics

For all statistical analyses, confirm that the following items are present in the figure legend, table legend, main text, or Methods section.

n/a	Confirmed	
☐	☒	The exact sample size (*n*) for each experimental group/condition, given as a discrete number and unit of measurement
☒	☐	A statement on whether measurements were taken from distinct samples or whether the same sample was measured repeatedly
☒	☐	The statistical test(s) used AND whether they are one- or two-sided *Only common tests should be described solely by name; describe more complex techniques in the Methods section.*
☒	☐	A description of all covariates tested
☒	☐	A description of any assumptions or corrections, such as tests of normality and adjustment for multiple comparisons
☐	☒	A full description of the statistical parameters including central tendency (e.g. means) or other basic estimates (e.g. regression coefficient) AND variation (e.g. standard deviation) or associated estimates of uncertainty (e.g. confidence intervals)
☒	☐	For null hypothesis testing, the test statistic (e.g. *F*, *t*, *r*) with confidence intervals, effect sizes, degrees of freedom and *P* value noted *Give P values as exact values whenever suitable.*
☐	☒	For Bayesian analysis, information on the choice of priors and Markov chain Monte Carlo settings
☒	☐	For hierarchical and complex designs, identification of the appropriate level for tests and full reporting of outcomes
☒	☐	Estimates of effect sizes (e.g. Cohen's *d*, Pearson's *r*), indicating how they were calculated

Our web collection on statistics for biologists contains articles on many of the points above.

Software and code

Policy information about availability of computer code

Data collection	The morphological features of the middle ear ossicles were observed under the microscope or interpreted from CT scans.
Data analysis	Phylogenetic Analysis was performed using TNT 1.5 (freely available from the Willi Hennig Society) and MrBayes 3.2.7 (open source); Bayesian MCMC runs were viewed in Tracer 1.7 (https://github.com/beast-dev/tracer/releases/latest); the clock rate was calculated using ape package (http://ape-package.ird.fr/) and the fitdistrplus package (https://github.com/aursiber/fitdistrplus) in R 4.0.3; the three-dimensional reconstructions were created using the software Mimics (version 16.1) and Amira-Avizo 2020.2.

For manuscripts utilizing custom algorithms or software that are central to the research but not yet described in published literature, software must be made available to editors and reviewers. We strongly encourage code deposition in a community repository (e.g. GitHub). See the Nature Research guidelines for submitting code & software for further information.

Data

Policy information about availability of data

All manuscripts must include a data availability statement. This statement should provide the following information, where applicable:
- Accession codes, unique identifiers, or web links for publicly available datasets
- A list of figures that have associated raw data
- A description of any restrictions on data availability

The data matrix for the phylogenetic analysis is deposited in MorphoBank (Project number 3760); CT data is deposited in MorphoSource (https://doi.org/10.17602/M2/M167344).

Field-specific reporting

Please select the one below that is the best fit for your research. If you are not sure, read the appropriate sections before making your selection.

☐ Life sciences   ☐ Behavioural & social sciences   ☒ Ecological, evolutionary & environmental sciences

For a reference copy of the document with all sections, see nature.com/documents/nr-reporting-summary-flat.pdf

Ecological, evolutionary & environmental sciences study design

All studies must disclose on these points even when the disclosure is negative.

Study description	Our study is based on a single fossil specimen, which is deposited in the Inner Mongolia Museum of Natural History, Inner Mongolia, China.
Research sample	Comparisons with other Mesozoic fossils were constrained by the number of specimens recovered for particular taxa; all were included where possible. Comparisons with extant mammals were conducted in the collections of the Section of Mammals, Carnegie Museum of Natural History, Pittsburgh, USA. The data matrix consists of 130 taxa and 509 characters.
Sampling strategy	The comparative sample was assembled to include purported close relatives of the fossil under study as well as representatives of the major mammalian lineages and outgroups.
Data collection	Data were collected by direct study of fossils and extant museum specimens or indirect study from the literature.
Timing and spatial scale	As the fossil understudy was Middle Jurassic in age, our comparative sample included primarily Mesozoic fossils along with extant mammals.
Data exclusions	As noted in the Supplementary Information, we excluded one Middle Jurassic fossil, Megaconus, from our comparative sample because of ongoing controversy about the interpretations of fundamental features of this fossil and because our team has not had the opportunity to study this fossil directly.
Reproducibility	Explicit phylogenetic methods allow other researchers to reproduce our study.
Randomization	NA, randomization is not applicable to our study.
Blinding	NA, blinding is not applicable to our study.

Did the study involve field work?   ☐ Yes   ☒ No

Reporting for specific materials, systems and methods

We require information from authors about some types of materials, experimental systems and methods used in many studies. Here, indicate whether each material, system or method listed is relevant to your study. If you are not sure if a list item applies to your research, read the appropriate section before selecting a response.

Materials & experimental systems

n/a	Involved in the study
☒ ☐	Antibodies
☒ ☐	Eukaryotic cell lines
☐ ☒	Palaeontology and archaeology
☒ ☐	Animals and other organisms
☒ ☐	Human research participants
☒ ☐	Clinical data
☒ ☐	Dual use research of concern

Methods

n/a	Involved in the study
☒ ☐	ChIP-seq
☒ ☐	Flow cytometry
☒ ☐	MRI-based neuroimaging

Palaeontology and Archaeology

Specimen provenance	The fossil was collected from the Tiaojishan Formation in Qinglong County, Hebei Province, China and the fossil collecting permit was obtained from the Department of Land and Resources, Inner Mongolia, China.
Specimen deposition	The fossil is accessioned in the collection of the Inner Mongolia Museum of Natural History, Inner Mongolia, China.
Dating methods	The age is based on stratigraphical correlation and previous radiometric data.

☐ Tick this box to confirm that the raw and calibrated dates are available in the paper or in Supplementary Information.

Ethics oversight | Research design and process followed the ethics guidelines of Carnegie Museum of Natural History and Indiana University of Pennsylvania.

Note that full information on the approval of the study protocol must also be provided in the manuscript.